Carbohydrate Polymers 106 (2014) 154–159

Contents lists available at ScienceDirect

Carbohydrate Polymers

journal homepage: www.elsevier.com/locate/carbpol

Facile and rapid thermo-regulated biomineralization of gold by pullulan and study of its thermodynamic parameters

Anirban Roy Choudhury[a,*], Ankit Malhotra[a], Paramita Bhattacharjee[b], G.S. Prasad[a]

[a] CSIR – Institute of Microbial Technology (IMTECH), Council of Scientific and Industrial Research, Sector 39A, Chandigarh 160 036, India
[b] Food Technology and Biochemical Engineering Department, Jadavpur University, Kolkata 700032, India

ARTICLE INFO

Article history:
Received 25 November 2013
Received in revised form 2 January 2014
Accepted 20 January 2014
Available online 7 February 2014

Keywords:
Pullulan
Biomineralization
Gold nanoparticles
Thermodynamics
Kinetics

ABSTRACT

A novel method for the production of gold nanoparticles (AuNPs) using pullulan as reducing and stabilizing agent has been developed. Quasi-spherical shaped AuNPs in the range of 50–100 nm were produced at three different temperature regimes 80 °C, 90 °C and 100 °C as characterized using UV–vis spectrophotometer, TEM and DLS. Study of reaction kinetics and thermodynamic parameters indicated that the reaction between pullulan and chloroauric acid for AuNPs formation followed first order reaction kinetics and higher temperature was favorable for the synthesis of smaller sized AuNPs. FT-IR data analyses, provided an insight towards the mechanism of gold nanoparticle formation which suggested that, the free $-CH_2OH$ groups of pullulan molecule were oxidized to carboxylate ions resulted in formation of AuNPs whereas the basic skeletal structure of pullulan remained unaltered. This study may open up new avenues for synthesis of tailor made biogenic AuNPs with possible application in biomedical field.

1. Introduction

Nanobiotechnology is growing at fast pace and considered as an emerging field for the development of metal nanoparticles. These metallic nanoparticles have drawn significant attention due to their unique physicochemical properties and potential for high end applications including medicine, electronics, imaging technology, optics and diagnostics (Sau, Rogach, Jackel, Klar, & Feldmann, 2010). Therefore, synthesis of nanoparticles with controlled shape and size with desired level of purity and yield is of utmost importance in the area of nano-science and technology. Predominantly, chemical and physical methods have been utilized for rapid synthesis of different metallic nanostructures including gold nanoparticles, silver nanocubes, zinc nanowires, copper nanotubes *etc.* (Chen, Chi, Zhang, Chen, & Chen, 2007; Sun & Xia, 2002; Yang et al., 2007). However, recent reports suggested that toxic effects of several harsh chemicals and solvents used in these type of methods have promoted utilization of biological agents for the synthesis of functional metal nanoparticles.

Mostly, soil and marine microflora and plant extracts were exploited to provide green route for the biosynthesis of different metal nanoparticles (Sharma et al., 2012). However, synthesis of nanoparticles using microbial and plant system is a slow process with low yield and often resulted in the production of polydisperse nanoparticles. Moreover, considering the cumbersome methodology and tedious process of down-streaming required to obtain nanoparticles using microbial and plant system, there is a need to develop a facile, green and rapid process for the synthesis of metal nanoparticles by utilizing materials that are non-hazardous and does not cause cellular toxicity. Polysaccharides may act as an ideal alternative to earlier reported biological agents (Park, Hong, Weyers, Kim, & Linhardt, 2011).

Offlate, polysaccharides, such as guar gum, starch, dextran, cellulose, and chitosan have been used as biological agents for production of gold nanoparticles (Engelbrekt et al., 2009; Huang & Yang, 2004; Pandey, Goswami, & Nanda, 2013; Uryupina, Ya Vysotskii, Matveev, Gusel'nikova, & Roldughin, 2011; Wang, Zhan, & Huang, 2010). However, all these polysaccharides have inherent problems of low solubility (Uryupina et al., 2011), high viscosity and also require derivitization and hence, cannot be employed in large scale production of gold nanoparticles (Ma, Yang, Li, & Yang, 2005; Park, Hong, Weyers, Kim & Linhardt, 2011). Moreover, requirement of additional stabilizing agents often make these processes more complex (Engelbrekt et al., 2009).

To address these challenges, a facile, rapid and green method for the synthesis of stable gold nanoparticles using pullulan as reducing and stabilizing agent was developed. The gold nanoparticles produced were characterized by measuring time dependent change in surface plasmon resonance (SPR) using UV–vis spectrophotometer, transmission electron microscopy (TEM) and dynamic light scattering (DLS). Further, a mechanism of gold nanoparticle formation

* Corresponding author. Tel.: +91 172 6665312; fax: +91 1722695215.
E-mail addresses: anirban@imtech.res.in, wb.anirban@gmail.com (A.R. Choudhury).

0144-8617/$ – see front matter © 2014 Elsevier Ltd. All rights reserved.
http://dx.doi.org/10.1016/j.carbpol.2014.01.072

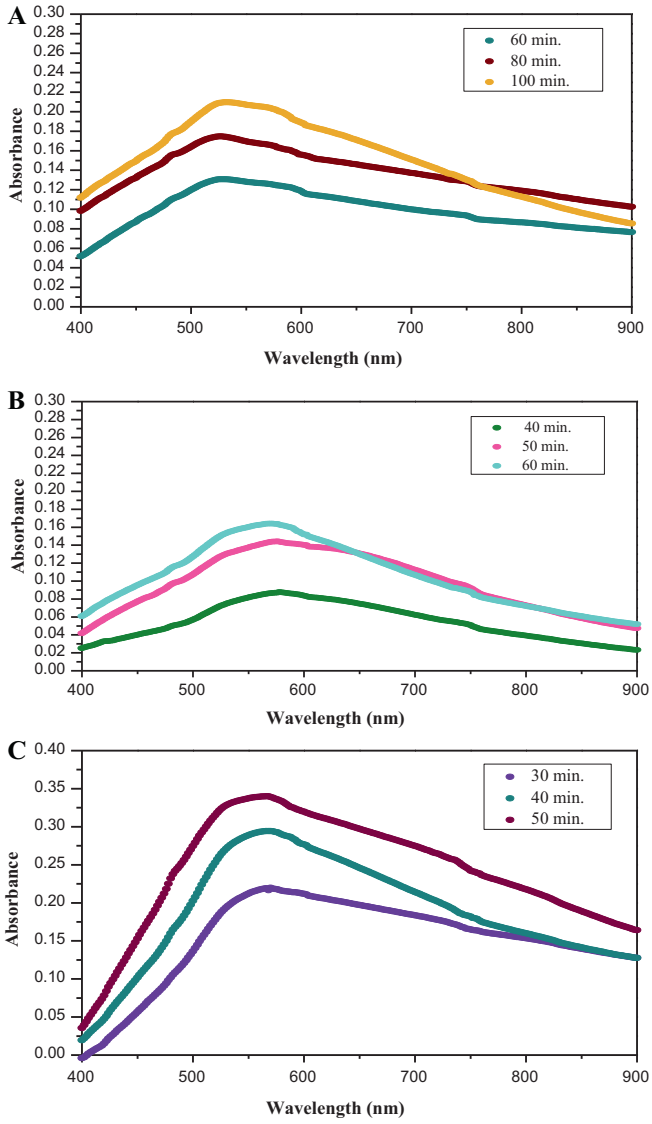

Fig. 1. Surface plasmon resonance data of gold nanoparticle formation after different time interval at (A) 80 °C (B) 90 °C (C) 100 °C.

and stabilization by pullulan has also been hypothesized based on comparative analysis of FT-IR data. The kinetics of formation of the gold nanoparticles has been investigated and the thermodynamic parameters such as Gibb's free energy, enthalpy and entropy have also been studied at different temperature regimes. To the best of our knowledge, this is the first report of gold nanoparticle synthesis using pullulan and also first attempt to understand the kinetic and thermodynamic parameters of metal nanoparticle formation using a biological agent.

2. Experimental

2.1. Synthesis of gold nanoparticles

To begin with the process of synthesizing gold nanoparticles, initially $HAuCl_4$ solution was made by adding weighed quantity of chloroauric acid (Loba Chemie Pvt. Ltd., India) in Milli-Q water. Further, pH of $HAuCl_4$ solution was adjusted to 5.3 by using 1 M NaOH (HiMedia Laboratories Pvt. Ltd., India) solution. Then, pullulan (Hayashibara Co. Ltd., Japan) was weighed accurately (0.5% w/v) and added directly to $HAuCl_4$ solution (250 mg/L, pH 5.3). The reaction mixture was incubated at three different temperatures

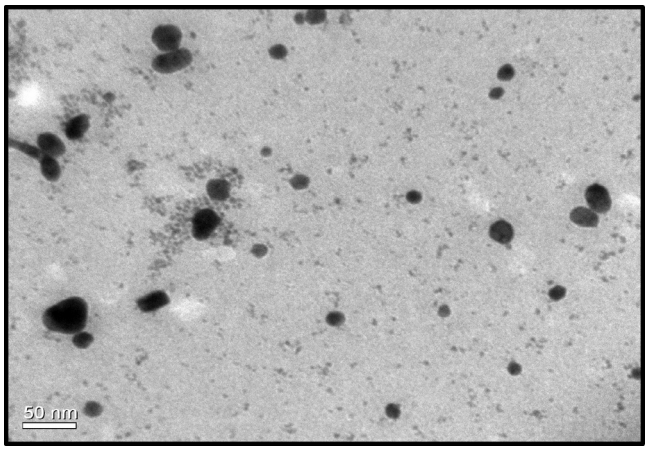

Fig. 2. Transmission electron micrograph of gold nanoparticles obtained at 100 °C illustrated quasi-spherical shaped nanoparticles.

(80 °C, 90 °C and 100 °C). Temperature regimes below 80 °C showed insignificant reaction rates and therefore higher temperature zones were investigated.

2.2. Characterization of gold nanoparticles

Spectral analysis of gold nanoparticles was carried out in a quartz cuvette of 1 mm path length by using HITACHI U2900 spectrophotometer. Scans were performed and SPR data were generated for samples obtained at different temperatures (80 °C, 90 °C and 100 °C) after regular time interval at a wavelength ranging 200–900 nm. Morphological analysis and particle size distribution of the nanoparticles produced under different conditions were studied using TEM and DLS as described by Malhotra et al. (2013). In addition, FT-IR spectra of both pure pullulan and pullulan stabilized gold nanoparticle were carried out in accordance to Kanmani and Lim (2013).

3. Results and discussion

3.1. Synthesis and characterization of gold nanoparticles

Synthesized gold nanoparticles were qualitatively analyzed by visual checking of color formation, appearance of purple color considered as the formation of gold nanoparticles. To further confirm the formation of gold nanoparticles in support of visual indication, quantitative analysis was performed by measuring time dependent variation in SPR using UV–visible spectrophotometer. Initially the reaction was carried out at room temperature and the rate of formation of gold nanoparticles was observed to be slow. Increase of temperature to 50 °C did not cause significant enhancement in the rate of reaction. Hence, time dependent SPR data were generated at elevated temperatures of 80 °C, 90 °C and 100 °C. Increase in absorption maxima was recorded during time course study in all the cases at different temperatures indicating increase in number of nanoparticles formation with time. Formation of gold nanoparticles starts after 60 min of incubation at 80 °C as indicated by the absorption maxima at 530 nm and plateau formation appeared after 90 min of incubation (Fig. 1A). At 90 °C, SPR showed formation of gold nanoparticles after 40 min of incubation with absorption maxima at 570 nm (Fig. 1B). Also, the fastest rate kinetics was observed at 100 °C where gold nanoparticles formation commenced after 30 min of incubation time and plateau appeared after 50 min of incubation with absorption maxima recorded at 570 nm (Fig. 1C). The overall data indicate that the AuNPs formed by pullulan showed maximum absorption at a wavelength

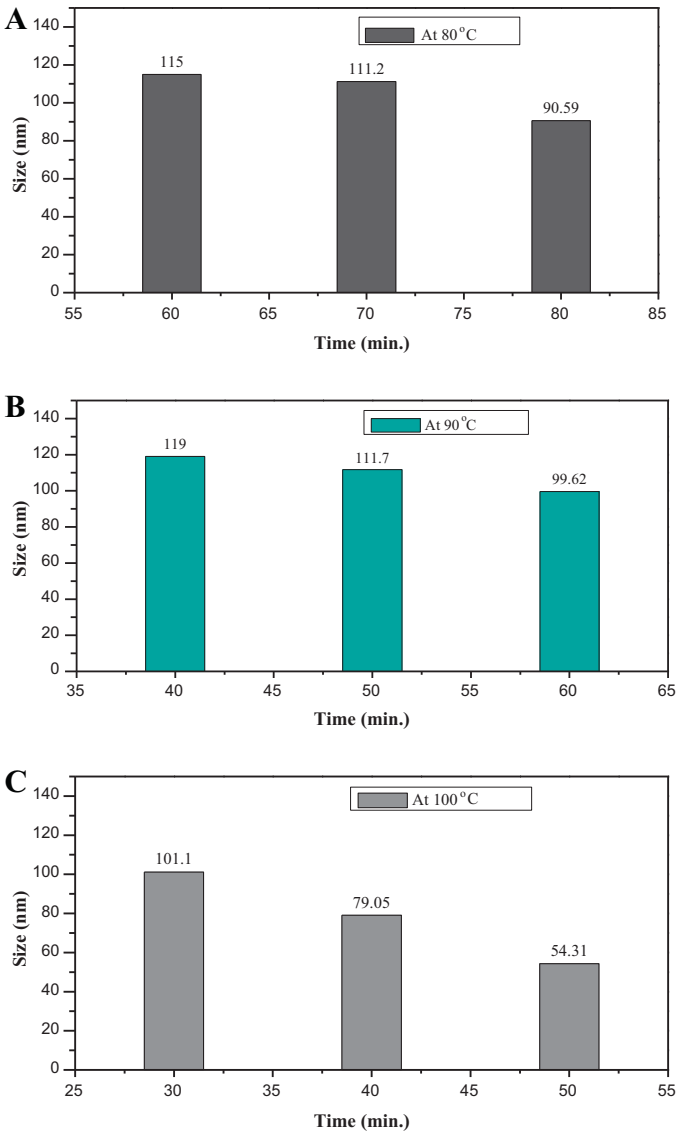

Fig. 3. DLS histogram represents average particle size of gold nanoparticle formation after different time interval at (A) 80 °C (B) 90 °C (C) 100 °C.

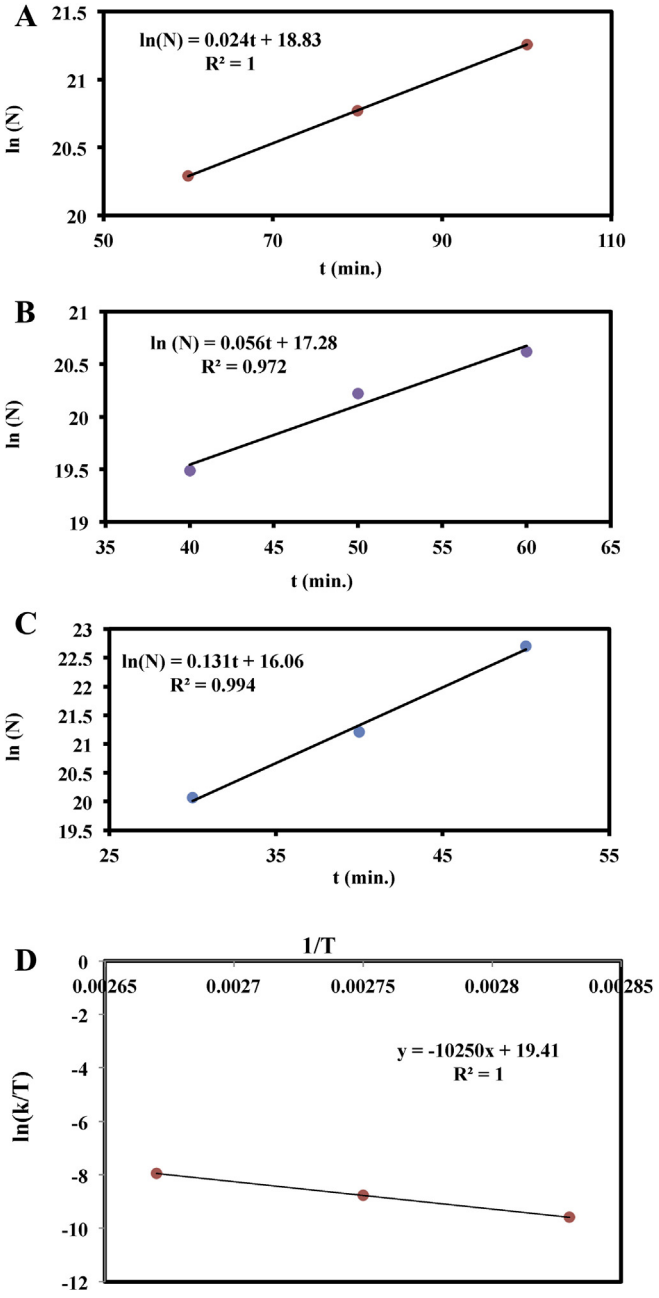

Fig. 4. Reaction kinetics of gold nanoparticle formation at (A) 80 °C (B) 90 °C (C) 100 °C. (D) Effect of different temperatures on the rate of gold nanoparticle formation using pullulan as reducing agent.

of 530 nm when the reaction was carried out at 80 °C. Similar absorption maxima were also reported for AuNPs formation using guar gum, another polysaccharide, as the reducing agent (Pandey et al., 2013). However in the present study, the absorption maxima shifted to 570 nm with an increase in incubation temperature. Earlier reports indicated that absorption maxima of AuNPs depends on several factors like size and shape of the nanoparticles (Rechberger et al., 2003) and may vary from 500 nm to 600 nm (Szunerits & Boukherroub, 2006). Therefore, a shift of the absorption maxima from 530 nm to 570 nm in the present case could be attributed to the difference in temperature of incubation, which resulted in the formation of variable size and shape gold nanoparticles. To investigate the morphology of gold nanoparticle, transmission electron microscopy imaging of a representative sample was performed at different magnifications. TEM micrograph of gold nanoparticle produced at 100 °C illustrated quasi-spherical shaped particles with particle size range between 50 and 100 nm (Fig. 2).

Furthermore, dynamic light scattering data were generated to understand the average size of gold nanoparticles. In all the cases, DLS data showed decrement in average size of particle with an increment in incubation time. Size of gold nanoparticles actually reduced from an average size of 115 nm to 90.59 nm at 80 °C (Fig. 3A), 119 nm to 99.62 nm at 90 °C (Fig. 3B) and 101.1 nm to 54.31 nm at 100 °C (Fig. 3C). This may be due to the fact that, at high temperature rate of reaction increases resulting in faster formation of gold nanoparticles with reduced nucleation/agglomeration. Moreover, viscosity of pullulan decreases with increase in temperature and thus could have acted as a better stabilizing agent for the gold nanoparticles formed. These two factors in combination may have resulted in formation of smaller sized gold nanoparticles at higher temperature.

3.2. Understanding the reaction kinetics and thermodynamic parameters of gold nanoparticle formation

Kinetics of gold nanoparticle formation was studied by quantifying the number of gold nanoparticles formed at a definite time

Table 1
Kinetic and thermodynamic parameters: change in Gibb's free energy, enthalpy and entropy at three different temperatures (80 °C, 90 °C and 100 °C) during the formation of gold nanoparticles.

Temperature (K)	Rate constant (s^{-1})	ΔG (J/mol)	ΔH (J/mol)	ΔS (J/K mol)
353.15	0.024	97,996.44		
363.15	0.056	98,358.12	85,223.72	−36.16
373.15	0.131	98,719.80		

interval using model equation developed by Haiss, Thanh, Aveyard, and Fernig (2007).

$$N = \frac{A_{450} \times 10^{14}}{d^2[-0.295 + 1.36\exp(-(d - 96.8/78.2)^2)]} \quad (1)$$

where, A_{450} is absorption maxima at wavelength 450 nm obtained by UV–visible spectrophotometer and d is an average particle diameter as measured by DLS.

Linear plots with R^2 values closer to 1 were obtained when graphs between two variables, ln (N) *vs* time (t) were constructed at three different temperatures *viz.* 80 °C (Fig. 4A), 90 °C (Fig. 4B) and 100 °C (Fig. 4C). These observations clearly illustrated that the gold nanoparticle formation using pullulan followed first order reaction kinetics. Rate constants of formation of gold nanoparticles at different temperatures were obtained from the slope of corresponding graphs. Interestingly, the rate constant values at different temperatures almost doubled with 10 °C increase in temperature in each case and thus followed Arrhenius equation of temperature dependence of rate of reactions (Table 1) (Laidler, 1987). Further, the rate constants were used for the determination of thermodynamic properties like Gibb's free

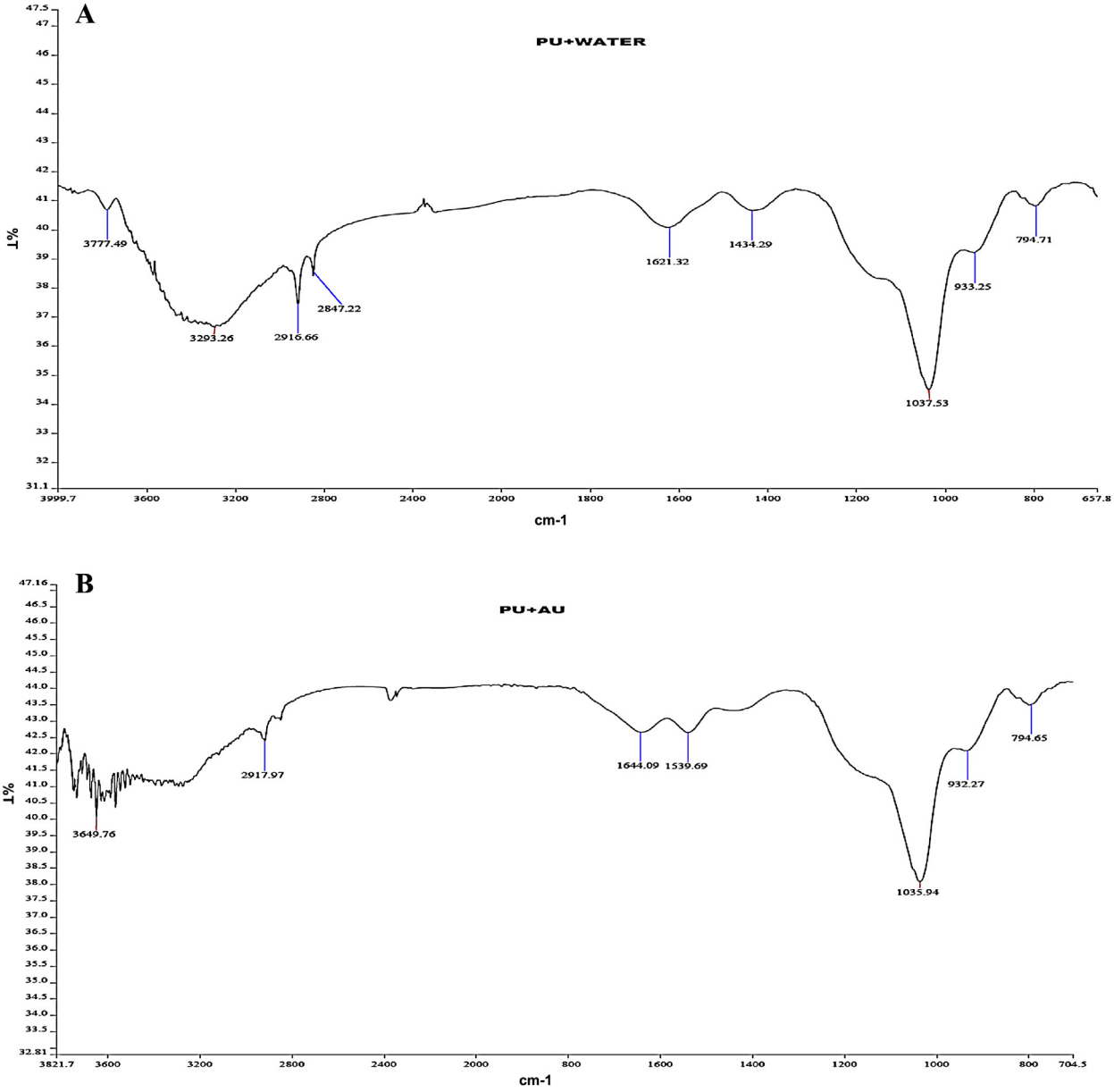

Fig. 5. (A) FT-IR spectra of pure pullulan. (B) FT-IR spectra of gold nanoparticles formed using pullulan.

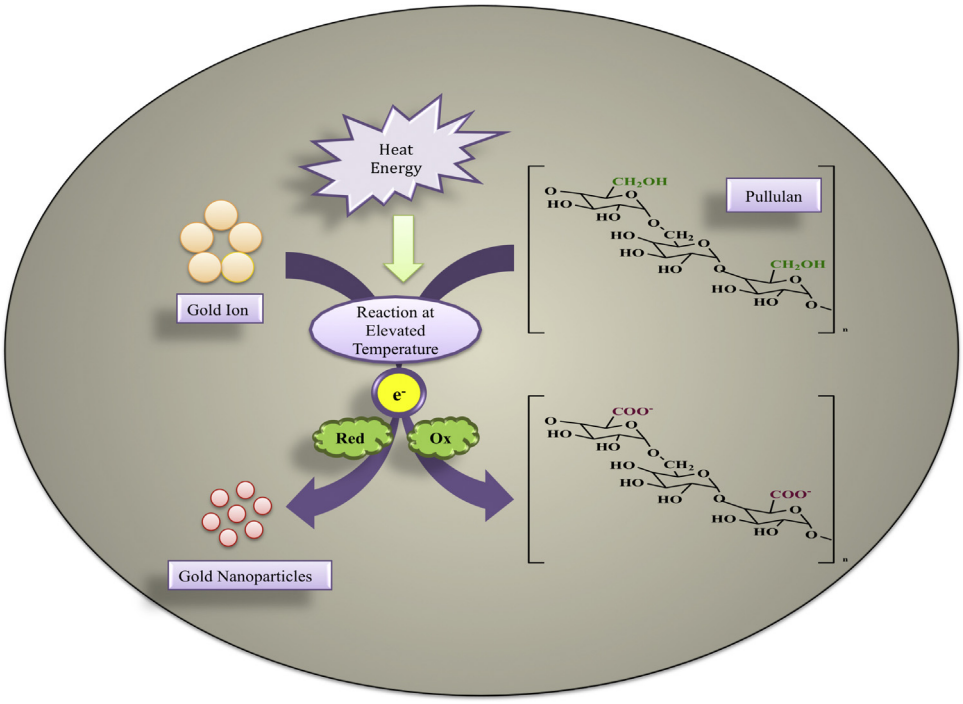

Fig. 6. Proposed mechanism of biomineralization of gold by pullulan.

energy, enthalpy and entropy changes which would facilitate in understanding energetics of gold nanoparticle formation using pullulan.

The change in rate of a chemical reaction with temperature may be described using Eyring's equation (Eyring, 1935). The linear form of Eyring's equation is as follows:

$$\ln\left[\frac{k}{T}\right] = \left[\frac{-\Delta H}{R}\right] \times \left[\frac{1}{T}\right] + \ln\left[\frac{k_B}{h}\right] + \left[\frac{\Delta S}{R}\right] \quad (2)$$

where, k is the reaction rate constant, T is the absolute temperature, ΔH is the change in enthalpy, R is the gas constant, k_B is the Boltzmann constant, h is the Plank's constant, ΔS is the change in entropy.

A plot of $[\ln(K)$ *vs* $1/T]$ was developed to obtain a linear fit with high regression coefficient (R^2) (Fig. 4D). Change in enthalpy (ΔH) during gold nanoparticle formation was obtained from the slope of this plot ($-\Delta H/R$), whereas, change in entropy (ΔS) was determined from the intercept of the plot $[\ln(k_B/h) + \Delta S/R]$ (Table 1). Similarly, changes in Gibb's free energy at different temperatures were calculated using the following equation:

$$\Delta G = \Delta H - T\Delta S \quad (3)$$

In this process, a positive change in enthalpy (ΔH) and negative change in entropy (ΔS) indicated that the process is non-spontaneous and can only takes place at higher temperature. Similarly, change in Gibbs free energy (ΔG) for the reaction was found to be positive, which also suggested that the reaction was feasible at higher temperature only (Table 1). Thus, the overall analysis of thermodynamic properties of pullulan mediated gold nanoparticle synthesis denoted that higher temperature would be more favorable for the reaction. More importantly a closer look at the data represented that higher temperature of incubation has resulted in increased number of gold nanoparticles production with lower average size demonstrating that higher temperatures supported faster and facile synthesis of gold nanoparticle when pullulan was used as stabilizing and reducing agent. Thus, it is imperative that, understanding of reaction kinetics and energetics of metal nanoparticle formation may aid in the development of a suitable process for the production of tailor made metal nanostructures.

3.3. FT-IR analysis and proposed mechanism of biomineralization of gold using pullulan as reducing agent

FT-IR spectra of pure pullulan and pullulan based gold nanoparticles were studied to investigate the participation of various functional groups of pullulan which act as reducing and stabilizing agents during the formation of the gold nanoparticles. FT-IR spectra of both samples clearly represent various characteristic peaks between 3650 cm^{-1} to 750 cm^{-1} (Fig. 5A and B). In either spectrum a strong absorption at 3649.76 cm^{-1} was observed indicating presence of O—H group. In addition, a sharp peak was observed at 2917.58 cm^{-1} corresponding to asymmetrical C—H stretching vibration, in accordance with the spectrum reported by Kanmani and Lim (2013). Furthermore, an absorption peak at 1643.36 cm^{-1} was observed that demonstrates stretching frequency of carbonyl group (C=O) (Kanmani & Lim, 2013). The characteristic absorption peaks of pullulan were observed between 750 cm^{-1} to 1050 cm^{-1} in FT-IR spectrum of both pure pullulan and pullulan mediated gold nanoparticles. This observation clearly indicated that the skeleton structure of pullulan remained unaltered during formation of gold nanoparticles and thus it could be concluded that, neither of α-1,4 and α-1,6 glycosidic linkages of pullulan was involved in the reaction leading to formation of AuNPs. However, minor shifts were observed in the absorption peaks in case of pullulan based gold nanoparticle spectrum as compared to the spectrum of pure pullulan. This minor shift of peaks may be attributed to the interaction of Au^{3+} with pullulan functional groups (Kanmani & Lim, 2013). Interestingly, a new peak was observed at 1539.11 cm^{-1} when pullulan–AuNPs spectrum was compared with pure pullulan spectrum. This absorption may be attributed to symmetric stretching vibrations of free carboxylate groups (Satyavani, Gurudeeban, Ramanathan, & Balasubramanian, 2011). Moreover, decrement in intensity of absorption peak at 1432.12 cm^{-1}, which corresponds to —C—H— bending for aliphatic —CH_2 was observed in pullulan–AuNP

spectrum (Parikh & Madamwar, 2006). Thus, it may be hypothesized that the free —CH_2OH— group of pure pullulan molecule was oxidized to carboxyl group (—COO^-), while concomitant reduction of Au^{3+} to Au^0 leading to the formation of gold nanoparticles (Fig. 6). These observations may be correlated with the formation of AuNPs using chitosan as reducing agent (Sun et al., 2008). However, in that case basic skeleton structure of chitosan was disrupted during the formation of gold nanoparticles whereas in present study FT-IR spectrum clearly indicated that formation of AuNPs using pullulan did not affect basic structure of pullulan and α-1,4 and α-1,6 linkages of pullulan remain intact during the reaction. Hence, it has been concluded that the fabrication of gold nanoparticles might be possible due to the oxidation of side chain aliphatic alcoholic group of pullulan moiety and further stabilization of pullulan–AuNPs can be supported by the interaction of other functional groups with gold.

4. Conclusion

In summary, a facile and rapid method has been established for the fabrication of biogenic gold nanoparticles using pullulan. Thermodynamic and kinetic study of gold nanoparticle formation showed that, the reaction was feasible at elevated temperature. More importantly, the rate of gold nanoparticle synthesis may be controlled using temperature as one of the major parameters. Further, a plausible mechanism of gold nanoparticle formation using pullulan has been provided. All these observations in combination unfold new pathways for the scientific community to develop processes for the production of tailor made biocompatible gold nanoparticles for promoting therapeutic applications.

Acknowledgements

This work was supported by grants from the Council of Scientific and Industrial Research (CSIR), Government of India. Authors would like to acknowledge Dr. Manoj Raje for providing TEM facility and Dr. Subash for providing technical assistance during TEM experiments.

References

Chen, Y. J., Chi, B., Zhang, H. Z., Chen, H., & Chen, Y. (2007). Controlled growth of zinc nanowires. *Materials Letters*, *61*, 144–147.

Engelbrekt, C., Sorensen, K. H., Zhang, J., Welinder, A. C., Jensen, P. S., & Ulstrup, J. (2009). Green synthesis of gold nanoparticles with starch–glucose and application in bioelectrochemistry. *Journal of Materials Chemistry*, *19*, 7839–7847.

Eyring, H. (1935). The activated complex in chemical reactions. *Journal of Chemical Physics*, *3*, 107–115.

Haiss, W., Thanh, N. T., Aveyard, J., & Fernig, D. G. (2007). Determination of size and concentration of gold nanoparticles from UV–vis spectra. *Analytical Chemistry*, *79*, 4215.

Huang, H., & Yang, X. (2004). Synthesis of chitosan-stabilized gold nanoparticles in the absence/presence of tripolyphosphate. *Biomacromolecules*, *5*, 2340–2346.

Kanmani, P., & Lim, S. T. (2013). Synthesis and characterization of pullulan-mediated silver nanoparticles and its antimicrobial activities. *Carbohydrate Polymers*, *97*, 421–428.

Laidler, K. J. (1987). *Chemical kinetics* (3rd ed., pp. 42). New York: Harper & Row.

Ma, Y., Yang, N., Li, C., & Yang, X. (2005). One-step synthesis of amino-dextran-protected gold and silver nanoparticles and its application in biosensors. *Analytical and Bioanalytical Chemistry*, *382*, 1044–1048.

Malhotra, A., Dolma, K., Kaur, N., Rathore, Y., Ashish, S., Mayilraj, S., & Choudhury, A. R. (2013). Biosynthesis of gold and silver nanoparticles using a novel marine strain of Stenotrophomonas. *Bioresource Technology*, *142*, 727–731.

Pandey, S., Goswami, G. K., & Nanda, K. K. (2013). Green synthesis of polysaccharide/gold nanoparticle nanocomposite: An efficient ammonia sensor. *Carbohydrate Polymers*, *94*, 229–234.

Parikh, A., & Madamwar, D. (2006). Partial characterization of extracellular polysaccharides from cyanobacteria. *Bioresource Technology*, *97*, 1822–1827.

Park, Y., Hong, Y. N., Weyers, A., Kim, Y. S., & Linhardt, R. J. (2011). Polysaccharides and phytochemicals: A natural reservoir for the green synthesis of gold and silver nanoparticles. *Nanobiotechnology*, *5*, 69–78.

Rechberger, W., Hohenau, A., Leitner, A., Krenn, J. R., Lamprecht, B., & Aussenegg, F. R. (2003). Optical properties of two interacting gold nanoparticles. *Optics Communications*, *220*, 137–141.

Satyavani, K., Gurudeeban, S., Ramanathan, T., & Balasubramanian, T. (2011). Biomedical potential of silver nanoparticles synthesized from calli cells of *Citrullus colocynthis* (L.) Schrad. *Journal of Nanobiotechnology*, *9*, 43.

Sau, T. K., Rogach, A. L., Jackel, F., Klar, T. A., & Feldmann, J. (2010). Properties and applications of colloidal nonspherical noble metal nanoparticles. *Advanced Materials*, *22*, 1805–1825.

Sharma, N., Pinnaka, A. K., Raje, M., Ashish, Bhattacharya, M. S., & Choudhury, A. R. (2012). Exploitation of marine bacteria for production of gold nanoparticles. *Microbial Cell Factories*, *11*, 86.

Sun, Y., & Xia, Y. (2002). Shape controlled synthesis of gold and silver nanoparticles. *Science*, *298*, 2176–2179.

Sun, C., Qu, R., Chen, H., Ji, C., Wang, C., Sun, Y., & Wang, B. (2008). Degradation behaviour of chitosan chains in the 'green' synthesis of gold nanoparticles. *Carbohydrate Research*, *343*, 2595–2599.

Szunerits, S., & Boukherroub, R. (2006). Electrochemical investigation of gold/silica thin film interfaces for electrochemical surface plasmon resonance studies. *Electrochemistry Communications*, *8*, 439–444.

Uryupina, O., Ya Vysotskii, V. V., Matveev, V. V., Gusel'nikova, A. V., & Roldughin, V. I. (2011). Production of gold nanoparticles in aqueous solutions of cellulose derivatives. *Colloid Journal*, *73*, 551–556.

Wang, Y., Zhan, L., & Huang, C. Z. (2010). One-pot preparation of dextran-capped gold nanoparticles at room temperature and colorimetric detection of dihydralazine sulfate in uric samples. *Analytical Methods*, *2*, 1982–1988.

Yang, D., Meng, G., Zhang, S., Hao, Y., An, X., Wei, Q., Ye, M., & Zhang, L. (2007). Electrochemical synthesis of metal and semimetal nanotube-nanowire heterojunctions and their electronic transport properties. *Chemical Communications*, *17*, 1733–1735.